

➤ **ORAL PRESENTATION**

**Influence of Shot Peening on Impact-Sliding Wear Behaviour of R260 Rail Steel**

Ahmet Deveci<sup>1</sup>(ORCID: <https://orcid.org/0000-0001-7378-6057>),  
Harun Mindivan<sup>1\*</sup>(ORCID: <https://orcid.org/0000-0003-3948-253X>)

<sup>1</sup>Bilecik Şeyh Edebali University, Engineering Faculty, Mechanical Engineering Department, Bilecik,  
Turkey

\*Corresponding author e-mail: [harun.mindivan@bilecik.edu.tr](mailto:harun.mindivan@bilecik.edu.tr)

**Abstract**

During operation, railway crossings are subjected to rolling, impact, and sliding stresses, with impact-sliding stress specifically occurring as the wheel transitions from the rail wing to the crossing nose. This transition generates extremely high contact forces on the crossing nose, which can cause significant damage to both the crossing nose and the wing rail. This study aims to present a technological approach for extending the service life of crossing noses manufactured from R260 rail steel. To investigate the mechanisms involved under complex loading conditions, wear tests were carried out using an inclined impact-sliding wear testing machine. In this study, shot peening (SP) was applied to R260 rail steel. The impact-sliding wear tests showed that the wear loss of the shot-peened R260 steel was noticeably lower compared to that of the untreated R260 steel at room temperature.

**Keywords:** R260 rail steel, Impact sliding wear, Shot peening.

**INTRODUCTION**

In railway transportation, the rail is a critical mechanical component that supports cyclic wheel loading and guides train movement. Continuous wheel loading makes the rail's surface layer vulnerable to wear and rolling contact fatigue (RCF) damage (Shen et al., 2022). These issues are especially pronounced in areas with small-radius curves, switches, and crossings. It is well established that rolling is the primary mode of wheel operation. However, during traction, braking, and turning, sliding wear caused by impacts between the wheel and rail plays a significant role in the degradation of the wheel/rail system (Chen et al., 2020). During service, impact-sliding occurs when the inclination of the rolling plane shifts from the wing rail to the crossing nose, where extremely high contact forces are exerted as the wheels pass over this area (Harzallah et al., 2012). In recent decades, substantial research has focused on improving the wear resistance and durability of rail steel to extend service life. Nevertheless, limited attention has been paid to the impact-sliding wear behavior of wheel/rail systems under conditions involving large contact and dynamic forces conditions that cause severe damage at crossings and produce contact stresses similar to those experienced in actual railway operations.

It is widely recognized that surface treatments such as shot peening, severe shot peening, re-shot peening, and precision grinding (Unal et al., 2022) as well as various coatings, can significantly improve the wear resistance and rolling contact fatigue (RCF) performance of rail materials (Peng et al., 2024). The shot peening (SP) process, categorized as a severe plastic deformation technique, is a well-established and effective surface treatment aimed at enhancing the metallurgical and mechanical properties, as well as the fatigue performance, of metallic materials under applied stresses. The process involves propelling hard steel balls at controlled velocities onto critical areas of a component's surface (Maleki and Unal, 2018).

Based on the above review, this study focused on developing a SP process for R260 rail steel under impact-sliding contact conditions. The process was performed at an Almen intensity of 24 A with a surface coverage of 600%. To replicate the extremely high contact and dynamic forces encountered in service, an inclined impact-sliding test method was employed (Zhao et al., 2017). Such conditions typically occur in regions where the rail transitions from the wing rail to the crossing nose, where the steel is exposed to combined impact and sliding forces during rolling-sliding contact. However, investigating crossing failures under cyclic high-speed impact-sliding motion remains a significant challenge due to the complex nature of tribological phenomena and dynamic loading effects.

## MATERIALS AND METHODS

Experimental tests were conducted on R260 rail steel, which was machined on a lathe without any additional heat treatment. The mechanically hardened layer was removed using silicon carbide paper up to 2000 grit. Grinding reduced the average surface roughness ( $R_a$ ) to 0.12  $\mu\text{m}$  prior to the SP process. The rail steel consists of pearlite with a hardness of 300 HV<sub>0.01</sub>.

The as-received R260 rail steels were subjected to SP using an industrial air blast machine (Sigma Shot Peening Company, Istanbul) under the parameters listed in Table 1. The process employed S230-grade steel shots (hardness range: 40-51 HRC) with a surface coverage of 600% to ensure thorough treatment of the steel surfaces. Peening intensity was measured using an Almen gauge with standard "Almen A" test strips, and the SP process was performed at an intensity of 24 A.

**Table 1.** SP conditions on R260 rail steel.

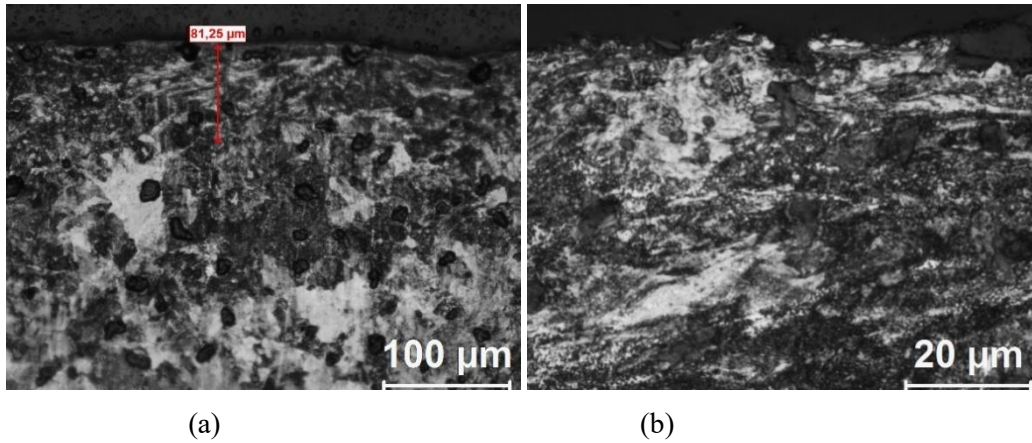
Treatment ID	SP Almen Intensity	Grinding Coverage (%)
24A-600	24A	600

After SP process, structural analysis of the cross-section of the shot-peened steel was performed using a light optical microscope (LOM, Nikon Eclipse LV150). The etching process was carried out by immersing the steels in a 2% nital solution for 15 seconds. The phases of the untreated and shot-peened steels were identified using an X-ray diffractometer (XRD, Panalytical Empyrean) with  $\text{CuK}_\alpha$  radiation, scanning over a  $2\theta$  range of  $30^\circ$  to  $110^\circ$ , with a step size of  $0.020^\circ$  and a scanning speed of  $1^\circ/\text{min}$ . Residual stress measurements were conducted using the fixed incident multiplane (FIM) technique, as described in detail by Sarioglu (Sarioglu, 2006). Surface roughness parameters ( $R_a$  and  $R_q$ ) were measured with a Mitutoyo contact profilometer (SJ-400 model) in accordance with the ISO 4287 standard. Microhardness was measured using a Shimadzu HMV tester with a 10 g load, at 10  $\mu\text{m}$  intervals up to a depth of 110  $\mu\text{m}$  from the surface on the polished cross-section.

Wear tests were conducted to evaluate the influence of SP process on the impact-sliding wear behavior of R260 rail steel. Prior to testing, a load cell was used to calibrate the maximum loads exerted by the spring and pneumatic cylinder to 40 N and 240 N, respectively. Each treated steel was subjected to 2000 impact cycles using a 10 mm diameter bearing steel (AISI 52100) ball under dry conditions ( $25 \pm 5^\circ\text{C}$ ,  $50 \pm 5\%$  relative humidity). Two distinct regions of the wear scar (impact and sliding) were examined using a 2D surface profilometer following the impact-sliding wear test to determine the amount of wear loss. Wear rates were calculated by dividing the volumetric wear loss by the number of loading cycles, expressed in  $\text{mm}^3/\text{cycle}$ . After the tests, LOM was employed to examine the wear tracks.

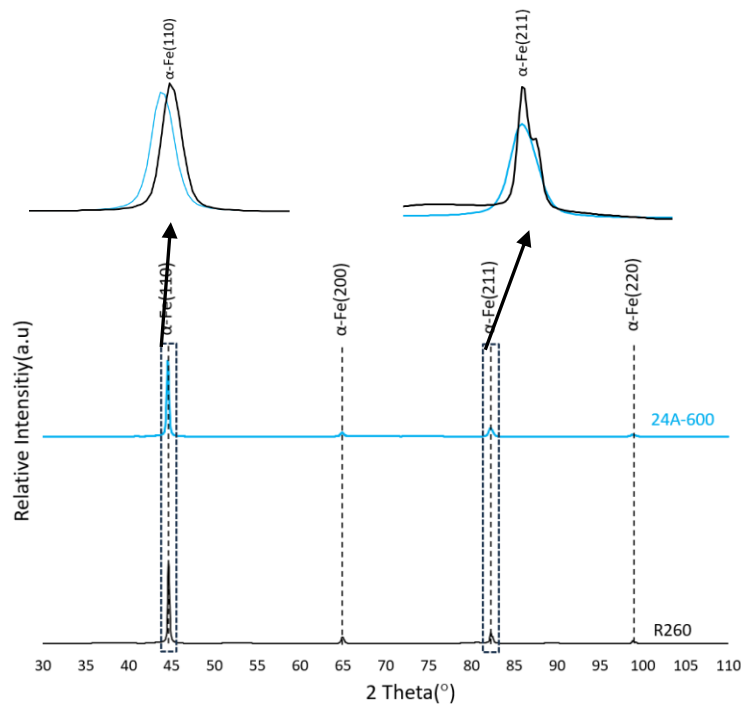
## RESULTS and DISCUSSION

Figure 1 depicts the LOM cross-sectional views of shot-peened R260 rail steel. It is evident that the standard shot peening parameters induced a moderate degree of plastic deformation within the surface layer, accompanied by microstructural refinement (Fig. 1). The deformation-affected layer exhibited a noticeable alignment of pearlite grains along with a reduction in their size.



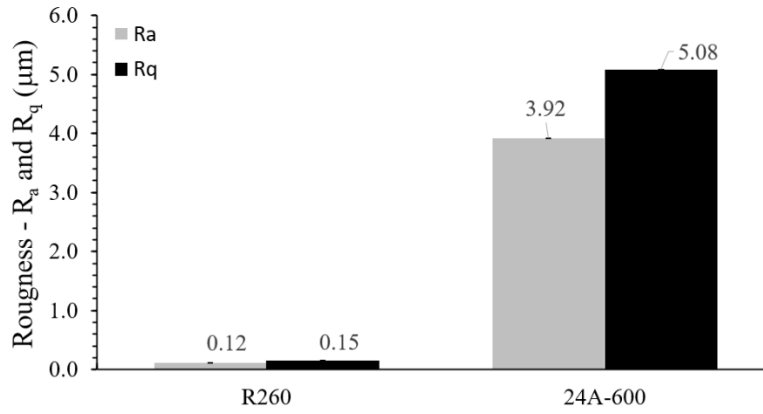
**Figure 1.** (a) Low and (b) high magnification LOM micrographs of the shot-peened R260 rail steel.

Figure 2 presents the XRD patterns of the surface layer for both untreated and shot peened steels. All steels displayed characteristic iron-based peaks ( $\alpha$ -Fe). In the shot peened steel, the  $\alpha$ -Fe peaks became broader, shifted to lower angles, and showed reduced intensity compared to the untreated steel. Additionally, the  $\alpha$ -Fe peaks in the shot-peened steels were broader and shifted to lower angles, suggesting grain refinement, increased lattice distortion, and the presence of compressive residual stresses resulting from higher dislocation density when compared to the untreated steel. By applying Bragg's law ( $n\lambda = 2d \sin \theta$ ), where  $d$  is the interplanar spacing,  $\theta$  is the diffraction angle,  $n$  is a positive integer, and  $\lambda$  is the XRD wavelength, the lattice parameters ( $a$ ) of both untreated and shot-peened steels were determined using the primary  $\alpha$ -Fe peak corresponding to the (110) diffraction plane. The calculated average lattice parameters were 0.287227 nm for the untreated steel and 0.287859 nm for the shot-peened steel. This represents a relative lattice expansion ( $\Delta a/a$ ) of about 0.22% in the shot-peened steel. Such an increase indicates the presence of greater compressive residual stress on the surface of the shot-peened steels, consistent with the findings modelled by Leskovšek et al. (Leskovšek et al., 2008).



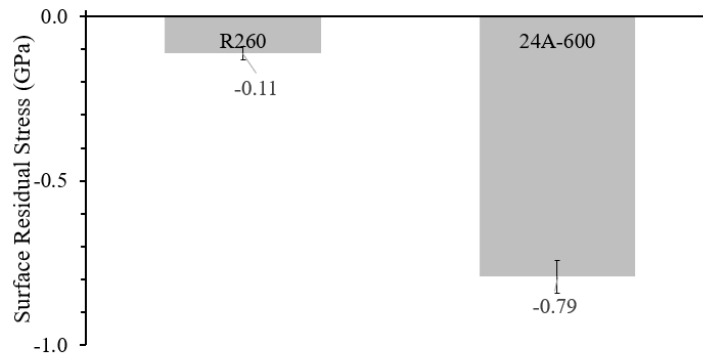
**Figure 2.** XRD patterns of the untreated and shot-peened steels.

Figure 3 shows the roughness values (parameters  $R_a$  and  $R_q$ ) measured before and after the SP process to investigate the influence of SP on the surface topography. The surface roughness generally increases by the plastic deformation capability and SP process raised the surface roughness.



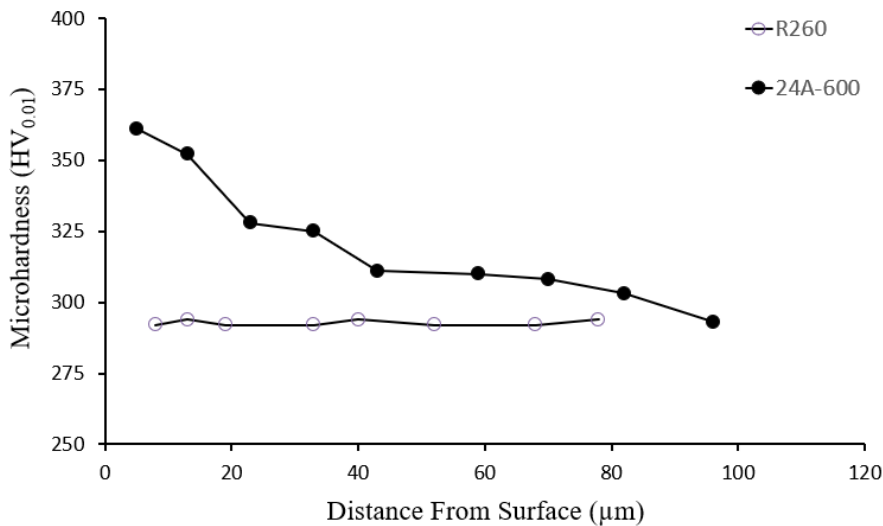
**Figure 3.** Surface roughness measurements of the the untreated and shot-peened steels.

Figure 4 illustrates the changes in compressive residual stress values for both untreated and shot-peened steels, measured using the FIM method. In the untreated steel, compressive residual stress was essentially absent, with values remaining near zero. Slight fluctuations were observed, likely due to prior machining or manufacturing processes such as casting and forming. In contrast, the shot-peened steel exhibited a significant increase in compressive residual stress approximately 618% higher than that of the untreated steel.



**Figure 4.** The residual stress state of the untreated and shot peened steels.

Figure 5 displays the microhardness distribution as a function of depth, providing insight into the thickness of the work-hardened layer. The untreated R260 rail steel exhibits a uniform base microhardness of approximately 300 HV<sub>0.01</sub>. In comparison, the shot-peened steel shows a gradual decrease in hardness with increasing depth. Notably, the surface microhardness of the shot-peened steel significantly increases to 361 HV<sub>0.01</sub> (about 1.2 times higher than that of the untreated steel) and the work-hardened layer extends to nearly 96  $\mu\text{m}$ .



**Figure 5.** Microhardness variation with depth for untreated and shot-peened steels.

Table 2 illustrates the wear track width and depth values of the impact and sliding zones for the untreated and shot-peened steels following impact-sliding wear tests. Both untreated and shot-peened steels exhibited deeper and wider wear tracks in the impact zone compared to the sliding zone. Figure 6 shows the average wear rates of the untreated and shot-peened steels in the impact and sliding zones. The wear rate in the impact zone decreased by 10% due to the SP process, while the wear rate in the sliding zone was reduced by approximately 11%. Overall, the SP treatment resulted in an approximately 11% decrease in the total wear rate.

**Table 2.** The wear track width and depth values of the impact and sliding zones of the wear tracks formed on the surfaces of the untreated and shot-peened steels.

		Impact Zone	Sliding Zone
R260	Wear Track Width	1.22 mm	1.07 mm
	Wear Track Depth	34.85 $\mu$ m	7 mm
24A-600	Wear Track Width	1.22 mm	1.00 mm
	Wear Track Depth	31.4 $\mu$ m	6.7 mm

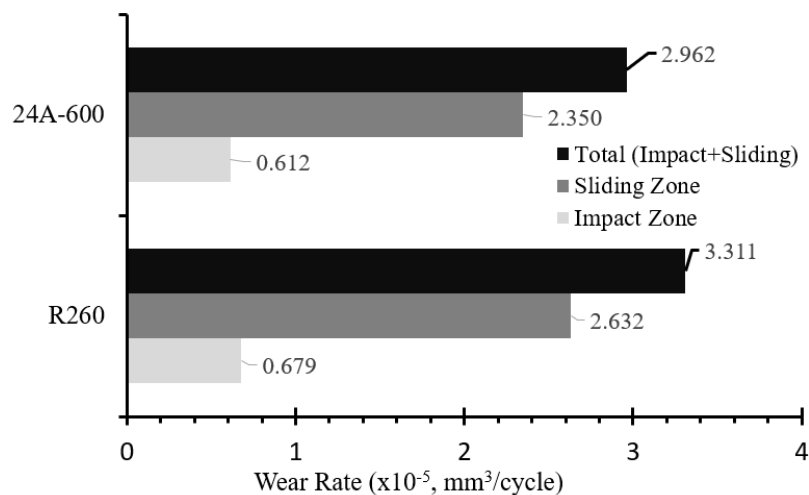


**Figure 6.** Wear rates of the wear tracks formed on the steels' surfaces.

Figs. 7 and 8 show detailed LOM images of the worn surfaces on the untreated and shot-peened steels. Results from the 2-D surface profilometer revealed that the shot-peened steel exhibited shallower wear tracks in both the impact and sliding zones (Table 2). Table 2 and Figure 5 suggest that the work-hardened layer in the shot-peened steel did not completely peel off in the impact zone. Additionally, wear tracks in both impact and sliding zones for untreated and shot-peened steels contained oxide patches (Figs. 7 and 8), a common indicator of tribo-oxidation caused by high frictional heat generated under elevated test loads (Peng et al., 2024). The observation of lateral cracks on the worn surface of the shot-peened steel at high magnifications suggests that fatigue is the predominant wear mechanism (Fig. 8). Upon impact, the untreated R260 steel exhibited a pronounced and deep crater on its surface (Table 2, Fig. 7). Although minor plastic deformation was observed, especially in the sliding zone of the untreated steel, the amount of surface fatigue wear cracks was significantly higher in the shot-peened steel, as depicted in Fig. 8. The shot-peened steel demonstrated strong resistance to deformation in both the impact and sliding zones within the work-hardened layer extending approximately 96  $\mu$ m from the surface (Fig. 5). The SP process may have induced greater compressive residual stress on the surface of the untreated R260 steel. Furthermore, SP caused elastic distortion in the R260 rail steel (approximately 0.22% for the shot-peened steel), leading to the formation of compressive residual stress, as modelled by Leskovšek et al. (Leskovšek et al., 2008). The shot-peened steel exhibited higher compressive residual stress (Fig. 4) and greater surface hardness (Fig. 5) compared to the untreated R260 rail steel.

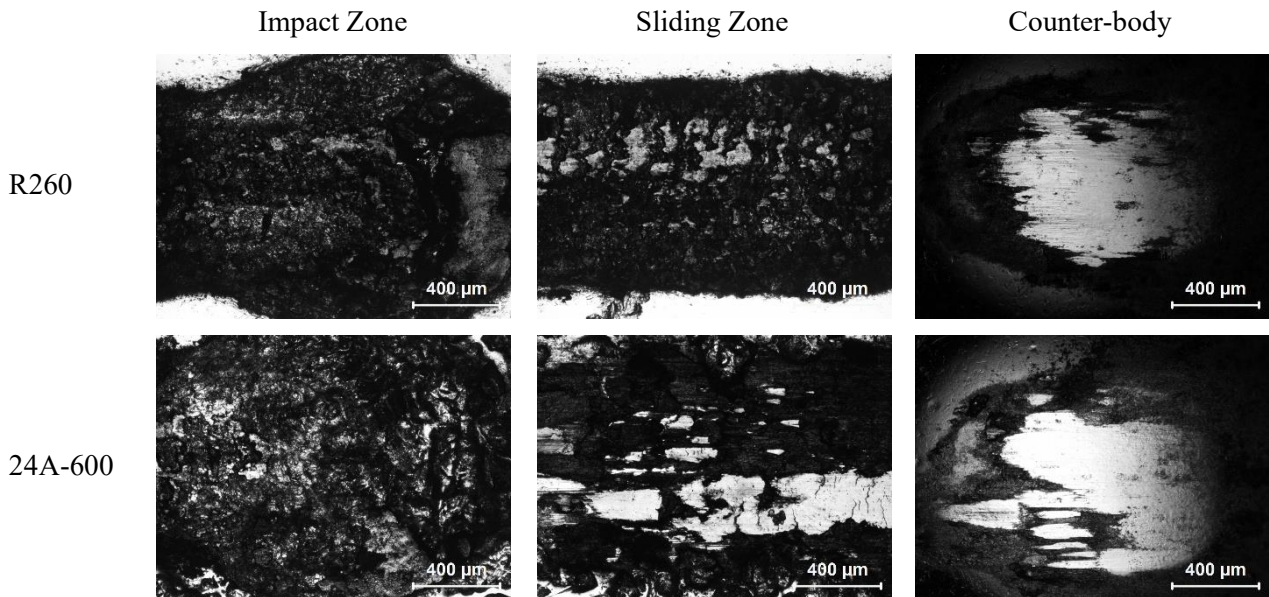


**Figure 7.** Low magnification LOM images of the wear tracks formed on the surfaces of the untreated and shot-peened steels, and LOM images of their corresponding testing balls after the wear test.

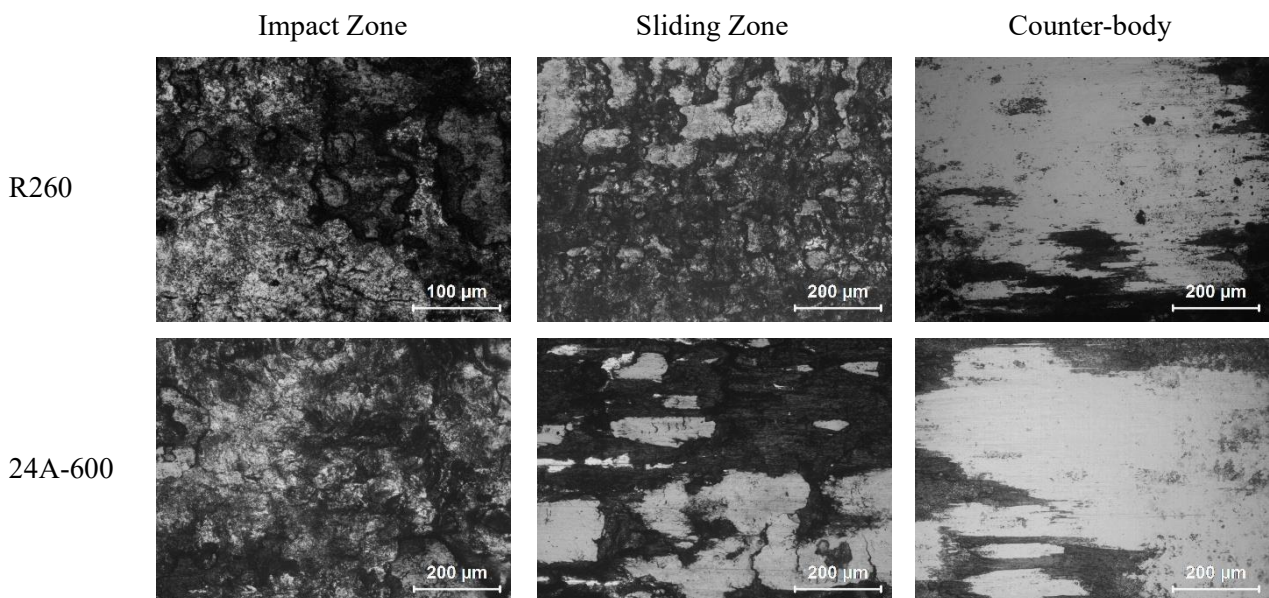


**Figure 8.** High magnification LOM images of the wear tracks formed on the surfaces of the untreated and shot-peened steels, and LOM images of their corresponding testing balls after the wear test.

## CONCLUSION

An inclined cyclic impact-sliding test was successfully employed to evaluate the fatigue wear behavior of untreated and shot-peened steels under extremely high contact stresses in ambient conditions. Based on the present study, the following conclusions can be drawn:

-The SP process produced a gradient structure characterized by high compressive residual stress and pronounced work hardening in the surface layer of R260 rail steel.

-The application of the SP process significantly increased the surface hardness of the untreated R260 rail steel. The surface hardness of the untreated and shot-peened steels was measured as 300 HV<sub>0.01</sub> and 361 HV<sub>0.01</sub>, respectively.

- The formation of greater lattice distortion on the surface of the shot-peened steel is accompanied by the generation of higher compressive residual stress compared to the untreated R260 rail steel
- The SP process increased the surface roughness of the untreated R260 rail steel.
- In the impact and sliding zones, the shot-peened steel exhibited 10% and 11% lower wear rates, respectively, compared to the untreated R260 rail steel under Hertzian contact pressures of 1.59/2.89 GPa.

## ACKNOWLEDGEMENTS

This work has been supported by Bilecik Şeyh Edebali University Scientific Research Projects Coordination Unit under grant number: 2023-01.BŞEÜ.03-02.

## REFERENCES

- Chen, Y., Gong, W., Kang, R. (2020). Review and propositions for the sliding/impact wear behavior in a contact interface. *Chinese Journal of Aeronautics*, 33(2), 391-406.
- Harzallah, R., Mouftiez, A., Hariri, S., Felder, E., & Maujean, J. P. (2012). Impact and sliding wear resistance of Hadfield and rail steel. *Applied Mechanics and Materials*, 146, 112-123.
- Leskovšek, V., Podgornik, B., & Nolan, D. (2008). Modelling of residual stress profiles in plasma nitrided tool steel. *Materials Characterization*, 59(4), 454-461.
- Maleki, E., & Unal, O. (2018). Roles of surface coverage increase and re-peening on properties of AISI 1045 carbon steel in conventional and severe shot peening processes. *Surfaces and Interfaces*, 11, 82-90.
- Peng, Y. X., Chang, X. D., Sun, S. S., Zhu, Z. C., Gong, X. S., Zou, S. Y., Xu, W.X., Mi, Z. T. (2018). The friction and wear properties of steel wire rope sliding against itself under impact load. *Wear*, 400, 194-206.
- Peng, K., Yu, D., Zhang, P., Xue, J., Li, Q., Wu, G., & Li, L. (2024). Mechanism and improvement of the rolling contact fatigue of the surface layer with heterogeneous microstructures of the rail steel treated by laminar plasma jet. *Engineering Failure Analysis*, 163, 108608.
- Sarioglu, C. (2006). The effect of anisotropy on residual stress values and modification of Serruys approach to residual stress calculations for coatings such as TiN, ZrN and HfN. *Surface and Coatings Technology*, 201(3-4), 707-717.
- Shen, M., Rong, B., Li, Q., Yu, M., Xiao, Y., & Zhao, H. (2023). Different responses of wheel–rail interface adhesion and wheel surface damage induced by an out–of–round wheel tread. *Wear*, 526, 204956.
- Unal, O., Maleki, E., Karademir, I., Husem, F., Efe, Y., & Das, T. (2022). Effects of conventional shot peening, severe shot peening, re-shot peening and precised grinding operations on fatigue performance of AISI 1050 railway axle steel. *International Journal of Fatigue*, 155, 106613.
- Zhao, C., Zhang, J., & Nie, X. (2017). Tribological behaviour of plasma nitrided cast iron D6510 and cast steel S0050A under the inclined-impact sliding condition with extremely high contact pressure. *Journal of Physics: Conference Series*. IOP Publishing, 843 (1), 1-9.